Minireview

Spectral imaging and its applications in live cell microscopy

Timo Zimmermann, Jens Rietdorf, Rainer Pepperkok*

Advanced Light Microscopy Facility and Cell Biology/Cell Biophysics Programme, European Molecular Biology Laboratory, Meyerhofstr. 1, D-69117 Heidelberg, Germany

Received 17 April 2003; revised 29 April 2003; accepted 29 April 2003

First published online 16 May 2003

Edited by Richard Marais

Abstract In biological microscopy, the ever expanding range of applications requires quantitative approaches that analyze several distinct fluorescent molecules at the same time in the same sample. However, the spectral properties of the fluorescent proteins and dyes presently available set an upper limit to the number of molecules that can be detected simultaneously with common microscopy methods. Spectral imaging and linear unmixing extends the possibilities to discriminate distinct fluorophores with highly overlapping emission spectra and thus the possibilities of multicolor imaging. This method also offers advantages for fast multicolor time-lapse microscopy and fluorescence resonance energy transfer measurements in living samples. Here we discuss recent progress on the technical implementation of the method, its limitations and applications to the imaging of biological samples.

Key words: Fluorescent protein; Multicolor microscopy; Fluorescence resonance energy transfer; Live cell imaging; Image analysis

1. Introduction

The completion of several genome sequencing projects now reveals many thousand open reading frames encoding novel proteins of unknown function. One of the major challenges but also opportunities in the next years will be to allocate functional data to each of these new proteins and to determine how they interact with each other to form the complex regulatory networks underlying fundamental processes of life and disease. Determining the sub-cellular localization and the dynamics of these novel proteins is one important step to be taken in order to bridge the gap between known sequence and unknown function. Another one will be to reveal the molecular interaction networks present in living cells and how this changes in space and time with respect to environmental or pathogenic alterations.

Multicolor fluorescence microscopy of living cells including advanced techniques such as fluorescence recovery after photobleaching, fluorescence correlation spectroscopy or fluorescence resonance energy transfer imaging (FRET) will be an essential tool in characterizing these novel proteins in their natural environment, the living cell [1–4]. Since the availability of genetically encoded fluorescent proteins (FPs) and their spectral variants [5–8], this has become much easier than ever before. Fluorescent labelling of virtually any protein in living cells is now possible by fusing the respective cDNA with the cDNA encoding a FP variant using simple molecular cloning methods and subsequent expression of the encoded fusion protein in cells. Although numerous different variants of FPs with distinct spectral properties are now available the number of proteins that can be simultaneously imaged in living cells involving FP variants is limited. The reasons are that many of the FPs suffer from drawbacks such as homo-oligomerization, slow folding properties or limited brightness. Furthermore, those FPs that have been most successfully applied in live cell imaging, such as CFP, GFP or YFP have strongly overlapping emission spectra which makes them difficult to separate in co-localization experiments using optical filtering methods. Usually, large amounts of the emitted fluorescence need to be discarded in order to achieve reliable dye separation. This is a major drawback when working with living cells, where as much fluorescence as possible should be collected in order to minimize the amounts of FPs that need to be expressed and the intensity of excitation light used, since both affect cell physiology. Recently, some progress has been made in order to improve the simultaneous detection of FPs by exploiting their distinct fluorescence lifetimes [9] to determine their relative contribution to each image pixel [10]. Fluorescence lifetime imaging has the advantage that most of the fluorescent light emitted by all FPs is collected, as only one dichroic mirror and emission filter is required in front of the detector. However, several images need to be taken in order to determine the fluorescence lifetimes which restrict the speed of image acquisition.

Here we discuss a further method, spectral imaging and subsequent linear unmixing, that has great potential for simultaneous imaging of FPs with strongly overlapping emission spectra.

2. Technical implementations of spectral imaging

Spectral imaging can be implemented in several ways on widefield or confocal microscopes. On a standard widefield fluorescence microscope, spectral separation of overlapping fluorophores could be improved quite simply by determining and correcting for the crossover of individual fluorophores into different filter sets [11,12]. Fourier transform spectroscopy has been implemented by coupling an interferometer to a

*Corresponding author. Fax: (49)-6221-1387 306.
E-mail address: pepperko@embl-heidelberg.de (R. Pepperkok).

0014-5793/03/$22.00 © 2003 Published by Elsevier Science B.V. on behalf of the Federation of European Biochemical Societies.
doi:10.1016/S0014-5793(03)00521-0

widefield microscope to obtain detailed spectral information at every position in a sample [13,14]. By subjecting such spectral image data to a linear unmixing analysis using singular value decomposition, up to seven fluorophores could be simultaneously imaged and distinguished [14]. The same linear unmixing strategy was also applied to spectral data obtained with a tunable filter on a two-photon confocal microscope to separate up to four FP variants [15]. These approaches acquire the spectral data sequentially as a series of images (λ-stack). This is time-consuming and requires up to several minutes to acquire one λ-stack. The methods further suffer from fluorophore specific photobleaching rates which become most significant in sequential image acquisition. This poses serious problems for imaging living samples where the localization of the FPs can rapidly change during data acquisition and photobleaching may cause unpredictable effects on cell physiology. These problems with sequential data acquisition can be overcome by subjecting the spectral information into parallel detection channels. This has now been implemented on commercial confocal microscopes such as the LSM510 Meta from Zeiss which uses a grating for the spectral dispersion of the signal onto a multidetector array [16,17]. Parallel acquisition of spectral image data has also been implemented on a prism-based spectral confocal microscope (Leica AOBS and SP systems [18], see also [19]).

For unmixing the spectral data, the relative contribution of each fluorophore to each detection channel needs to be available as a reference λ-stack (see Fig. 1, also called spectral profile). Since this is determined by the spectral properties of the respective fluorophores and is independent of their

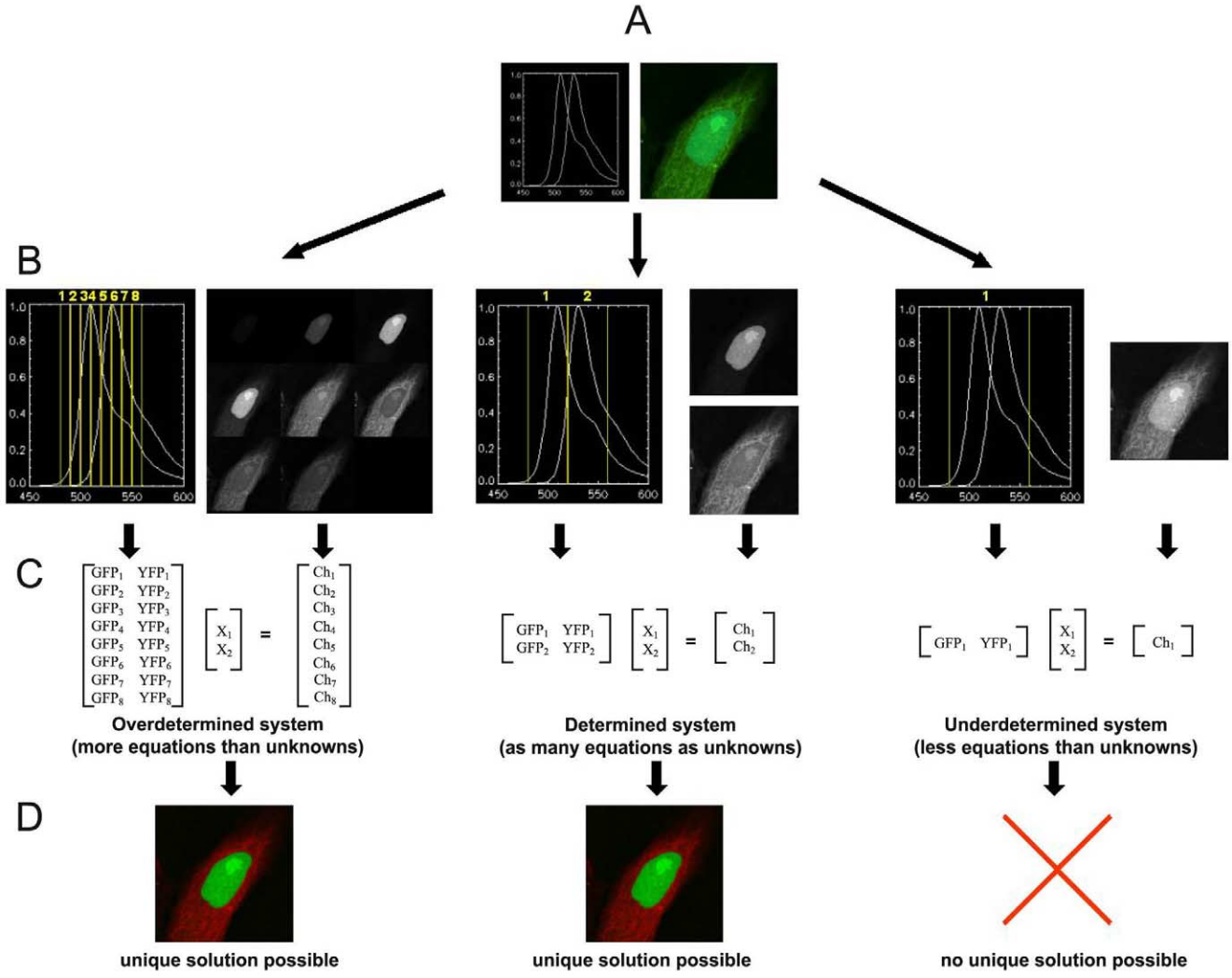

Fig. 1. Steps in linear unmixing outlined for a sample expressing EGFP- and YFP-tagged fusion proteins. The cells shown express EGFP with a nuclear localization signal in the nucleus and YFP-labelled tubulin. A: On the left image the spectra of EGFP and YFP and on the right image cells as perceived in the microscope are shown. EGFP and YFP fluorescence both appear green and can thus not be distinguished by eye. B: The respective detection channels (yellow) are indicated in the plots of the spectra and the image contributions to the individual detection channels are displayed next to them as a gallery. C: In the unmixing formulas, which need to be applied to every pixel in the acquired images, the normalized spectral contributions of EGFP or YFP to each channel derived from the reference λ-stack are expressed as GFP_n and YFP_n. The unknown contributions of GFP and YFP to be determined are expressed as X_1, X_2, respectively. The pixel specific gray values derived from the acquired images of cells are expressed as Ch_n. D: Images after linear unmixing. GFP is shown in green and YFP in red. B, C, D left column: the number of detection channels (eight) exceeds the number of fluorophores (two) and linear unmixing of EGFP and YFP is possible. B, C, D middle column: the number of detection channels (two) matches the number of fluorophores (two) and represents the minimum number of detection channels required to allow linear unmixing of EGFP and YFP. B, C, D right column: one detection channel is not sufficient to distinguish EGFP and YFP and a unique solution of the equations is impossible.

concentrations, the reference λ-stacks can be used to assemble a matrix of fluorophore specific weighting factors, that is subsequently used to determine the contribution of each fluorophore to each image pixel (see for example [14] or [15]). When the number of detection channels exceeds the number of fluorophores to be separated, the system is mathematically overdetermined and unmixing is possible. When the number of detection channels equals the number of fluorophores to be separated the system is just determined and a unique solution of the unmixing procedure is possible. This means that for two closely related fluorophores two detection channels are sufficient for efficient unmixing (see Figs. 1 and 2). This has the advantage that the two fluorophores might even be excited with only one wavelength (for example at 488 nm for EGFP and YFP, Fig. 2A–F) and simultaneously detected with two detection channels that can even be arranged on one detector such as a CCD camera. The benefit of such a simple set-up for spectral imaging and unmixing is that the data can be rapidly collected, as no part of the microscope needs to be moved, and the two color channels are acquired simultaneously which is a prerequisite for ratiometric measurements as they are common for ion imaging or FRET analyses by sensitized emission.

The same concept used for the linear unmixing of emission spectra can also be applied to unmixing based on the fluorophore's excitation spectra. Instead of exciting at one wavelength and collecting the emitted fluorescence into spectrally different detection channels, one can excite sequentially at different wavelengths and detect the total respective fluorescence with only one detector. Data acquired in such a way can then be unmixed with the same algorithm used for emission-based unmixing (see Fig. 2G–L). Such implementation of spectral unmixing should be ideal on set-ups equipped with excitation sources that allow fast switching of the excitation

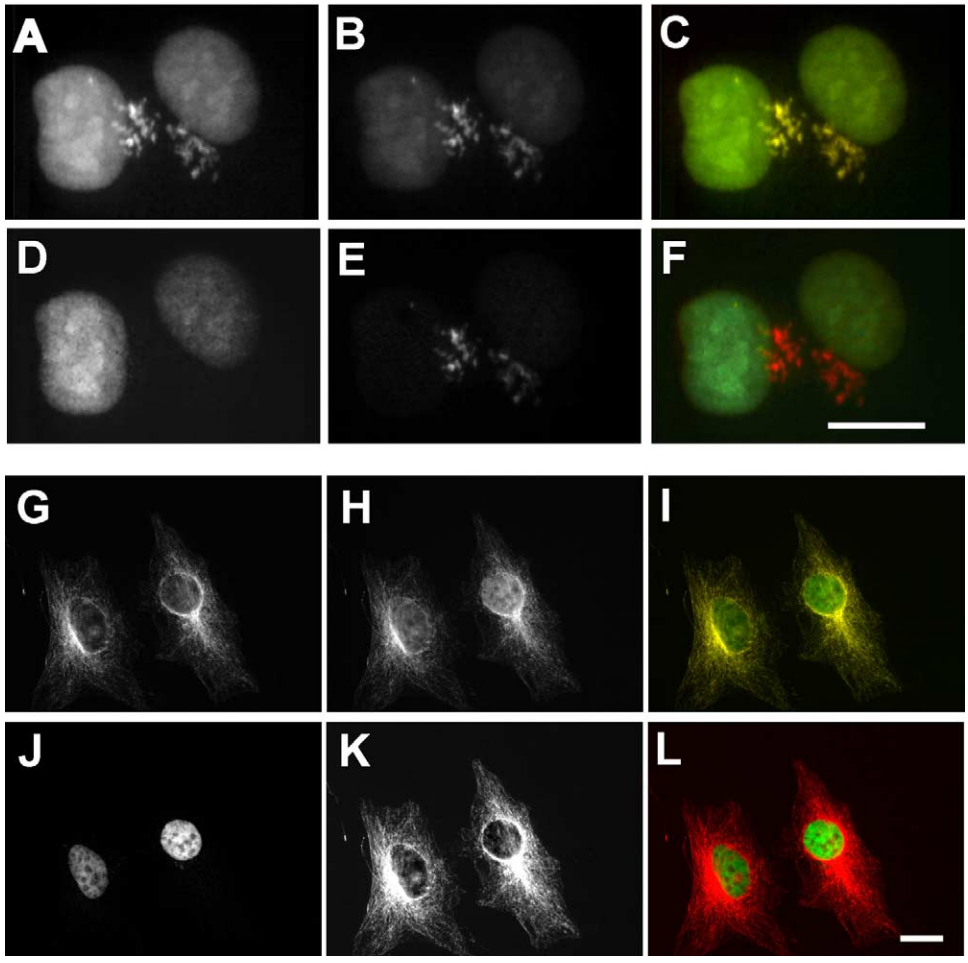

Fig. 2. A–F: In vivo imaging of EGFP and YFP fusion proteins using parallel detection and subsequent emission unmixing. Two-channel images were acquired simultaneously on a Perkin Elmer spinning disc confocal microscope equipped with an emission beam splitter (DualView, OpticalInsights Inc.). The sample was excited at 488 nm with an ArKr laser and the fluorescence signal was split into two channels detecting the 505–530 nm and 530–565 nm range, respectively. Nuclei are labelled with histone-EGFP and the Golgi complex with a Golgi-targeted YFP (from Clontech). Shown are projections of an acquired 3D stack. A–C: Images before unmixing. A: Detection channel 1, 505–530 nm. B: Detection channel 2, 530–565 nm. C: Overlay of the channels in (A) and (B) before linear unmixing. D–F: Fluorophore signals after unmixing. D: Histone-GFP in the nucleus. E: YFP in the Golgi. F: Overlay of (D) and (E) after linear unmixing. Image intensities were scaled in order to suit the presentation. G–L: Excitation-based unmixing of HeLa cells containing histone-GFP and Alexa 488-stained microtubules. The sample was imaged on a widefield microscope with just one emission filter (530/50) and beamsplitter (500) under two different excitations using autoexposures. G: Image taken with a 475/40 excitation filter. H: Image taken with a 436/20 excitation filter. I: Overlay image of the two channels without linear unmixing. The crosstalk of the Alexa 488-labelled microtubules is clearly visible as yellow. J–L: Images of the cells after linear excitation unmixing. J: Histone-GFP. K: Alexa 488-labelled microtubules. L: Overlay image of the unmixed fluorophores. Scale bars = 10 μm.

light. Since the number of fluorophores, that can be separated by linear unmixing, is limited by the number of channels available for analysis (see Fig. 1), combining excitation and emission unmixing increases the number of fluorophores that could be imaged in parallel.

3. Limitations

Spectral imaging is an established method in the field of satellite imaging and remote sensing and thus the factors affecting efficiency have already been thoroughly considered

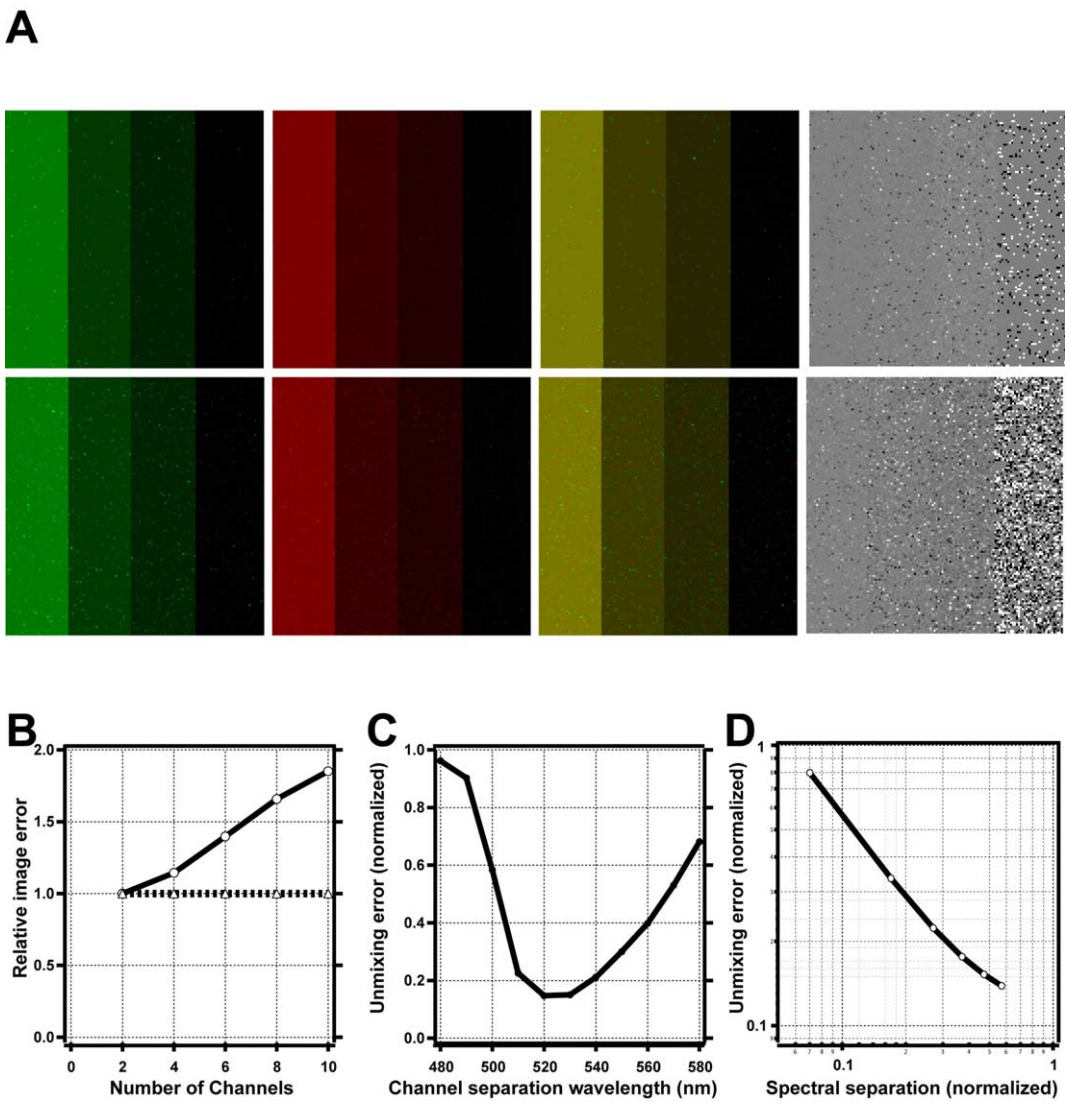

Fig. 3. Examples of factors influencing the efficiency of spectral unmixing. The simulation data were created and processed with routines written in Interactive Data Language (Research Systems, Inc.). A: Influence of detector noise and the number of channels on unmixing efficiency. For this purpose, test datasets of simulated EGFP (green) and YFP signals (red) of varying intensities were generated and combined with empty images acquired on a Zeiss LSM510 confocal microscope under speed and sensitivity settings suitable for in vivo imaging. These background images introduce realistic readout noise into the simulated images. The created gray values in the EGFP and YFP images are identical and thus co-localize with a 1:1 ratio in every image pixel and thus the signals appear in the overlay images (third column) as yellow. The number of detectors covering the spectral range between 460 and 580 nm was either set to two (top row, each channel with a 60 nm bandwidth) or 10 channels (bottom row, each channel with a 12 nm bandwidth). The unmixing error for two and 10 channels can be visualized in a ratio image (gray scale) of the unmixed EGFP and YFP images. Correctly unmixed pixels should have values of 1.0 (gray) whereas deviations are visible as darker or brighter pixels. The ratio image created with two channels (top row) contains less noise errors than the image created with 10 channels (bottom row). As can be seen for the stripes of different intensities, the errors become more significant for weaker intensities in the image. B: Dependence of unmixing efficiency on the number of detection channels in the absence and presence of detector noise. The relative increase of the unmixing error is independent of the actual noise level. Image error values in the graph are normalized to the image error obtained for two channel unmixing. Solid line with circles: relative image error in the presence of detector noise. Broken line with triangles: relative image error without noise. C: Influence of detection channel characteristics on the unmixing exemplified for two detection channels. An EGFP signal was simulated and unmixed against YFP with detector noise added. Moving the border between the two detection channels to different wavelengths demonstrates the existence of an optimal position corresponding to minimal unmixing error. D: Dependence of the image error on the amount of overlap of the fluorophore spectra. For this, two emission spectra resembling that of EGFP were simulated, unmixed (two detection channels) and the unmixing error determined at conditions with varying spectral separation of the two created emission spectra. The spectral separation was normalized in such a way that total overlap with the spectra represents 0 and total separation of the spectra represents 1. The unmixing error decreases with increasing spectral separation.

[20]. The method is predominantly limited by factors such as image background or detector noise, but the appropriate selection of the number and bandwidth of the detection channels with respect to the overlap of the fluorophores to be distinguished also plays an important role. These limitations become most critical when imaging living specimen, where the signals of interest are usually weak.

3.1. Background

Removing any signal not originating from the fluorophores to be analyzed by background subtraction is an essential prerequisite for the linear unmixing analysis [14]. As with ratiometric measurements [21], failure to correct the background properly leads to significant intensity-dependent artefacts in the processed images. However, in cases of spectrally homogeneous background, there is the option to treat the background as a further fluorophore and thus separate it from the specimen specific fluorescent signals by linear unmixing.

3.2. Noise

Since linear unmixing is a pixel-based method it is susceptible to errors introduced into the original images or the reference spectra by the Poisson noise of the fluorescence signal itself and the detector readout noise. These sources of noise become important at low light levels in live specimens imaging where usually the illumination light and exposure time have to be kept at a minimum in order to preserve the physiological integrity of the sample. Computer simulations show that in the absence of noise unmixing efficiencies are independent of the number of detection channels used (Fig. 3B). However, in the presence of detector readout noise, the errors in the processed image increase relative with the number of detection channels (Fig. 3A,B). The reasons for this are that for a fixed detector readout noise the signal to noise ratio (SNR) will decrease according to $1/n$ (n = number of detection channels) for each detector. This decrease of the SNR is only partially compensated by the noise averaging effect that occurs due to the increased number of detection channels (improvement according to $n^{-1/2}$, see [22]). Consequently, the SNR decreases according to $n^{-1/2}$ and thus sampling the spectral information into few detection channels with a broad bandwidth should result in superior quality of the unmixed data compared to sampling into a large number of detection channels with narrow bandwidths.

3.3. Detector channel arrangements and spectral overlap of the fluorophores

If the spectra of the fluorophores to be imaged are known from independent measurements, then an optimized arrangement of the detector channels to obtain a maximum SNR can be calculated (see Fig. 3C). However, even with optimized channel settings, the unmixing efficiency is directly affected by the amount of spectral overlap between the fluorophores. In the absence of noise, the degree of overlap does not affect unmixing efficiency. However, in the presence of noise the errors of the unmixed data increase with the spectral overlap of the fluorophores (Fig. 3D). One way to overcome this is by over-sampling, which has been nicely exploited on a widefield microscope by applying sequential imaging with detection filter arrangements partially overlapping in sequential acquisitions [23].

4. Biological applications

An obvious advantage of spectral imaging compared to conventional microscopy methods is the increased number of distinct fluorescent molecules that can be simultaneously detected [14,15]. With the recent availability of commercial confocal microscopes that allow spectral imaging and linear unmixing the number of such applications will drastically increase in the future. The method opens however a variety of additional possibilities that go beyond the increase of the number of fluorescent markers that can be imaged in parallel.

Because of the highly dynamic nature of processes in living samples, it is essential for in vivo co-localization experiments or ratiometric methods to gather information of two or more fluorescent molecules at the same time. With GFP-tagged proteins this is usually difficult to achieve due to the lack of spectral variants that can be excited simultaneously but do not bleed through significantly in the emission channels. Further complications arise when the need to resolve fast processes, such as the movement of membrane transport carriers [24], precludes the use of time-consuming sequential image acquisition which can overcome bleed through problems with GFP variants to some extent [25]. For these problems, spectral imaging offers the possibility to excite two spectrally similar fluorophores, for example EGFP and EYFP, with just one wavelength (e.g. 488 nm) and detect them simultaneously without significant losses of the emitted fluorescence (Fig. 2A–F). In contrast to common methods involving glass filters to separate the emitted light from distinct fluorophores, spectral imaging collects almost all of the fluorescence emitted, which is critical for work with living samples. Thus spectral imaging, even with only two fluorophores being involved, should always be the method of choice when working with living samples.

A further application of spectral imaging is in FRET microscopy, which is an important tool for imaging the dynamics of cellular processes like protein–protein interactions or post-translational modifications [3]. However, an efficient FRET signal requires significant overlap between the emission spectrum of the donor and the excitation spectrum of the acceptor fluorophore. This requirement is inevitably accompanied by a significant overlap of the emission spectra of the donor and acceptor and complicates the determination of FRET efficiencies [3,26]. As spectral imaging is well suited to separate even highly overlapping donor and acceptor emissions, FRET imaging with already established donor acceptor pairs can be facilitated [17] and applied to so far not used FP-based donor acceptor pairs with increased FRET efficiencies due to the increased spectral overlap of the donor emission and acceptor excitation [19].

5. Conclusions

Spectral imaging and linear unmixing is an approach that overcomes a number of limitations of common fluorescence microscopy methods aiming at the parallel detection of several fluorescent molecules at the same time. Since almost all of the fluorescence emitted can be collected by this method without compromising the discrimination between distinct fluorescent molecules, it offers increased sensitivity, which is critical when working with living samples. It also allows the use of FPs that could not be imaged and discriminated so far in parallel and

thus extends not only our abilities and performance of multicolor imaging, but also the use of more efficient donor acceptor fluorophore pairs for FRET imaging.

Acknowledgements: We thank Peter Verveer for continuous discussions, Leica (Mannheim, Germany), Olympus (Hamburg, Germany) and Perkin Elmer Life Science (Cambridge, UK) for support of the Advanced Light Microscopy Facility at EMBL Heidelberg and Brigitte Joggerst for excellent technical assistance. Our laboratory is supported by a Quality of Life EU Network Grant QCRI-CT-2002-01272 and by BMBF Grants Nos. 01 KW0013 and 01GR0101.

References

[1] White, J. and Stelzer, E. (1999) Trends Cell Biol. 9, 61–65.
[2] Medina, M.A. and Schwille, P. (2002) BioEssays 24, 758–764.
[3] Wouters, F.S., Verveer, P.J. and Bastiaens, P.I. (2001) Trends Cell Biol. 11, 203–211.
[4] Bastiaens, P.I. and Pepperkok, R. (2000) Trends Biochem. Sci. 25, 631–637.
[5] Chalfie, M., Tu, Y., Euskirchen, G., Ward, W.W. and Prasher, D.C. (1994) Science 263, 802–805.
[6] Cubitt, A.B., Heim, R., Adams, S.R., Boyd, A.E., Gross, L.A. and Tsien, R.Y. (1995) Trends Biochem. Sci. 20, 448–455.
[7] Zhang, J.C.R., Ting, A.Y. and Tsien, R.Y. (2002) Nat. Rev. Mol. Cell Biol. 3, 906–918.
[8] Matz, M.V.L.K. and Lukyanov, S.A. (2002) Bioessays 24, 953–959.
[9] Pepperkok, R., Squire, A., Geley, S. and Bastiaens, P.I. (1999) Curr. Biol. 9, 269–272.
[10] Verveer, P.J.S.A. and Bastiaens, P.I. (2000) Biophys. J. 78, 2127–2137.
[11] Castleman, K.R. (1994) Bioimaging 2, 160–162.
[12] Kato, N., Pontier, D. and Lam, E. (2002) Plant. Physiol. 129, 931–942.
[13] Malik, Z., Cabib, D., Buckwald, R.A., Talmi, A., Garini, Y. and Lipson, S.G. (1996) J. Microsc. 182, 133–140.
[14] Tsurui, H., Nishimura, H., Hattori, S., Hirose, S., Okumura, K. and Shirai, T. (2000) J. Histochem. Cytochem. 48, 653–662.
[15] Lansford, R., Bearman, G. and Fraser, S.E. (2001) J. Biomed. Opt. 6, 311–318.
[16] Dickinson, M.E., Bearman, G., Tilie, S., Lansford, R. and Fraser, S.E. (2001) Biotechniques 31, 1272–1278.
[17] Hiraoka, Y., Shimi, T. and Haraguchi, T. (2002) Cell Struct. Funct. 27, 367–374.
[18] Olschewski, F. (2002) Imag. Microsc. 4, 22–24.
[19] Zimmermann, T., Rietdorf, J., Girod, A., Georget, V. and Pepperkok, R. (2002) FEBS Lett. 531, 245–249.
[20] Landgrebe, D. (2000) Hyperspectral Image Data Analysis, IEEE Sig. Proc. Mag.
[21] Bolsover, S.R., Silver, R.A., Whitaker, M. (1993) Ratio Imaging Measurement of Intracellular Calcium and pH, in: Electronic Light Microscopy (Shotton, D., Ed.), pp. 181–210, Wiley-Liss, New York.
[22] Sheppard, C.J.R., Gu, M. and Roy, M. (1992) J. Microsc. 168, 209–218.
[23] Garini, Y., Gil, A., Bar-Am, I., Cabib, D. and Katzir, N. (1999) Cytometry 35, 214–226.
[24] Shima, D.T., Scales, S.J., Kreis, T.E. and Pepperkok, R. (1999) Curr. Biol. 9, 821–824.
[25] Ellenberg, J., Lippincott Schwartz, J. and Presley, J.F. (1999) Trends Cell Biol. 9, 52–56.
[26] Gordon, G.W., Berry, G., Liang, X.H., Levine, B. and Herman, B. (1998) Biophys. J. 74, 2702–2713.